Adaptive Quantized Fault-Tolerant Control for a Riser-Vessel System With Unknown Control Direction and Input Saturation

Xiaowei Wang, Baoshan Zhang, Shouyan Chen, Limin Wang, Zhijia Zhao, *Member, IEEE*, Zhijie Liu, *Member, IEEE*, and Keum-Shik Hong, *Life Fellow, IEEE*

***Abstract*—With the burgeoning growth of the maritime economy, marine risers have emerged as reliable and convenient conduits for the transport of oil and natural gas. However, these risers are vulnerable to vibrational disturbances, which can adversely impact system performance and induce fatigue damage. Therefore, effective vibration control strategies are required to address this issue. This study introduces an innovative adaptive quantized fault-tolerant control strategy designed to attenuate vibrations in a three-dimensional (3-D) riser-vessel system against the effects of actuator faults, unknown control direction, and external disturbances. Different from previous findings, the suggested controller can directly counteract the nonlinear component stemming from actuator faults and handle the nonlinear decomposition inherent to the quantizer, without the necessity for upper-limit estimation. Furthermore, to tackle the input saturation, control laws are formulated using the hyperbolic tangent operator. Finally, the proposed controller's effectiveness and robustness are validated through thorough Lyapunov analysis and numerical simulations, affirming the system's uniformly bounded stability.**

***Index Terms*—Actuator fault, adaptive quantized control, input saturation, riser-vessel system, unknown control direction.**

Received 28 April 2024; accepted 20 October 2024. Date of publication 25 November 2024; date of current version 16 January 2025. This work was supported in part by the National Natural Science Foundation of China under Grant 62273112, Grant 62433011, Grant 62163012, and Grant 62473039; in part by the Guangdong Basic and Applied Basic Research Foundation under Grant 2023B1515120018 and Grant 2023B1515120019; in part by the Science and Technology Planning Project of Guangzhou, China, under Grant 2023A03J0120; and in part by the National Research Foundation of Korea funded by the Ministry of Science and ICT, South Korea, under Grant IRIS-2023-00207954. This article was recommended by Associate Editor R. Cui. *(Corresponding authors: Shouyan Chen; Zhijia Zhao.)*

Xiaowei Wang, Shouyan Chen, Limin Wang, and Zhijia Zhao are with the School of Mechanical and Electrical Engineering, Guangzhou University, Guangzhou 510006, China (e-mail: meewxw_ee@gzhu.edu.cn; maxcsy@gzhu.edu.cn; lm_wang@gzhu.edu.cn; zhjzhaoscut@163.com).

Baoshan Zhang is with the Science and Technology Research and Development Department, Henan Nengchuang Electronic Technology Company, Ltd., Guangzhou 510000, China (e-mail: wai307@163.com).

Zhijie Liu is with the School of Intelligence Science and Technology, University of Science and Technology Beijing, Beijing 100083, China (e-mail: liuzhijie@ustb.edu.cn).

Keum-Shik Hong is with the Institute for Future, School of Automation, Qingdao University, Qingdao 266071, China, and also with the School of Mechanical Engineering, Pusan National University, Busan 46241, South Korea (e-mail: kshong@pusan.ac.kr).

Color versions of one or more figures in this article are available at https://doi.org/10.1109/TSMC.2024.3487257.

Digital Object Identifier 10.1109/TSMC.2024.3487257

I. Introduction

In THE context of the rapidly expanding maritime economy and growing emphasis on ocean energy resource development [1], ensuring the efficiency and reliability of offshore petroleum and natural gas extraction presents a significant challenge within the field of offshore engineering. Flexible marine risers have gained prominence as efficient, swift, cost-effective, and reliable means for the offshore transport of hydrocarbons. Nevertheless, the inherent flexibility renders them vulnerable to generating vibrations and deformations in dynamic marine environments. Such excessive vibrations can compromise the operational performance of these risers and lead to fatigue-related damage. Consequently, the formulation of effective vibration control strategies has emerged as a pressing concern requiring immediate attention.

Marine risers exemplify an engineering application of flexible structures, prompting the development of various control techniques to attenuate their vibrations. Among these methods, boundary control has demonstrated significant advantages over distributed control and model simplification, requiring fewer sensors and actuators while avoiding spillover effects [2], [3]. In recent years, advancements in boundary control for flexible structures have merged. In [4], a boundary control was established to enable a flexible wing to follow a desired trajectory by manipulating two angles. In [5], a boundary control law featuring input and output constraints was proposed, which were designed using a smooth hyperbolic tangent operator (HTO) and a barrier Lyapunov function. A boundary controller designed for the tail-end connection was reported to regulate the oscillations of flexible tails [6]. In [7], an effective boundary control was proposed for a flexible robotic manipulator to achieve the goals of disturbance rejection and angle tracking. However, these prior studies focused primarily on suppressing vibrations in flexible structures, and these methods are not directly applicable to three-dimensional (3-D) riser-vessel systems with input saturation.

In industrial settings, control systems frequently confront a range of constraints arising from factors, such as gear clearance, power limitations, and valve capacities. Consequently, these constraints must be incorporated when devising vibration control strategies for flexible marine riser systems. Among various input constraints, such as dead zones, backlash, and hysteresis, input saturation emerges as a predominant issue in practical applications [8]. Excessive

control input rates can compromise the actuator's ability to meet the system's dynamic requirements, thereby adversely affecting its performance. Therefore, investigating the issue of control input saturation in practical mechanical systems is of considerable significance. In [9], a resilient adaptive fixed-time sliding-mode control was formulated for robotic systems encountering parameter uncertainties and input saturation. In [10], a proposed adaptive fuzzy control strategy addresses output-constrained switched stochastic nonlinear systems while considering input saturation. In [11], a novel boundary control strategy was developed to minimize vibration offsets, and an auxiliary term was introduced to address input saturation constraints. An effective fault-tolerant control (FTC) system was developed for networked flexible manipulators to address actuator failures, input saturations, and external disturbances in [12]. Although significant developments have been attained in addressing the input saturation of flexible systems, no studies have explored the use of the HTO to mitigate input saturation specifically in 3-D flexible riser systems. This research gap serves as the impetus for the current study.

Uncertainty regarding the signs and magnitudes of coefficients linked to control inputs in system models is termed unknown control directions, and it is a common and practical engineering challenge. In riser systems, the control signal output from the controller typically passes through a gain amplifier before being transmitted to the actuators. However, the performance of the amplifier can be affected by component aging or temperature variations, which can alter the direction of the control signal. In situations where immediate replacement of the amplifier is not feasible, sudden changes in the control direction can lead to system instability. In severe cases, it may result in oil leaks that could harm the marine environment. Therefore, we specifically consider scenarios where the control directions of riser systems are unknown. To date, research into unknown control directions of flexible systems described by partial differential equations has been relatively sparse [13]. In [14], a customized adaptive fuzzy tracking control was developed for switched multi-input–multioutput (MIMO) nonlinear systems, characterized by time-varying full state constraints and unknown control directions. In [15], the tracking control issue was explored in a class of MIMO nonlinear systems, accounting for both input saturation and unknown control direction gains. Successful solutions for the control of nonlinear systems with unknown control directions have been established, but a quantized control design for the 3-D flexible riser-vessel systems with unknown control directions is yet to be developed.

Quantized control is a methodology employed to represent and modulate control signals using discrete values, and has garnered significant interest across disciplines like engineering and automation. Quantized control offers the dual advantage of reducing communication rates while maintaining control stability, thus attracting substantial research attention in recent years [16]. Parallel distributed compensation event-triggered dynamic output quantization control was considered for the discrete-time switched Tagaki–Sugeno (T–S) fuzzy systems in [17]. A synthesized control approach was introduced, incorporating input and output quantizations to address nonlinear systems with mismatched parametric uncertainties using backstepping design, as documented in [18]. A co-design strategy was put forward to simultaneously determine the event-triggered parameter and the quantization scheme in [19]. While successful solutions have been offered for the robust control of nonlinear systems facing unknown direction or input quantization, the quantized control design for a 3-D flexible riser-vessel system with unknown direction, actuator faults, and input saturation remains unexplored, which drives further investigation.

This study aims to develop a new adaptive quantized FTC scheme for uncertain riser-vessel systems with unknown control direction and input saturation. The primary contributions are as follows.

1) Distinct from traditional adaptive FTC frameworks, the effective factor ρ and quantizer parameter δ can be directly compensated by the Nussbaum function, without the need to estimate their boundaries.
2) Leveraging the HTO, the proposed controller effectively mitigates vibrations and ensures system stability, all while adhering to the constraints on control inputs.
3) Remarkably, the controller maintains the convergence of system states without inducing spillover effects, even when confronted with challenges, such as input saturation, actuator faults, input quantization, and unknown control directions.

II. Problem Statement

A. System Model

The 3-D riser-vessel system depicted in Fig. 1 is characterized by the independent variables of time t, space z, and riser length l. The unit of t is seconds, and the unit of z is meters. The displacements of the riser in F, G, and H directions are denoted by $f(z,t)$, $g(z,t)$, and $h(z,t)$, respectively. Additionally, $\Gamma_f(z,t)$, $\Gamma_g(z,t)$, and $\Gamma_h(z,t)$ represent distributed disturbances in the riser system along the three directions. Unknown boundary disturbances acting on the vessel are expressed as $\Theta_f(t)$, $\Theta_g(t)$, and $\Theta_h(t)$. The boundary control inputs in F, G, and H directions are denoted as Φ_f, Φ_g, and Φ_h, respectively. For simplicity, several notations are defined as follows: $\mathcal{R}$ denotes a collection of real numbers, $(\star) = (\star)(z,t)$, $\dot{(\star)}$ is the partial derivative of $\star$ with respect to time, $(\star)'$ is the partial derivative of $\star$ with respect to space, $\dot{(\star)}'$ is the second partial derivative of $\star$ with respect to both space and time, $(\star)''$ is the second partial derivative of $\star$ with respect to space, $(\star)'''$ is the third partial derivative of $\star$ with respect to space, $(\star)''''$ is the fourth partial derivative of $\star$ with respect to space, $\ddot{(\star)}$ is the second partial derivative of $\star$ with respect to time, $(\star)_l = (\star)(l,t)$, and $(\star)_0 = (\star)(0,t)$.

Following the works [20], the dynamics of the riser-vessel system structure can be mathematically formulated as:

$$m\ddot{f} = Tf'' - EIf'''' + EA\left(h''f' + f''h'\right) + \frac{3}{2}EA\left(f'\right)^2 f'' + \frac{1}{2}EA\left[f''\left(g'\right)^2 + 2f'g'g''\right] + \Gamma_f, 0 < z < l \tag{1}$$

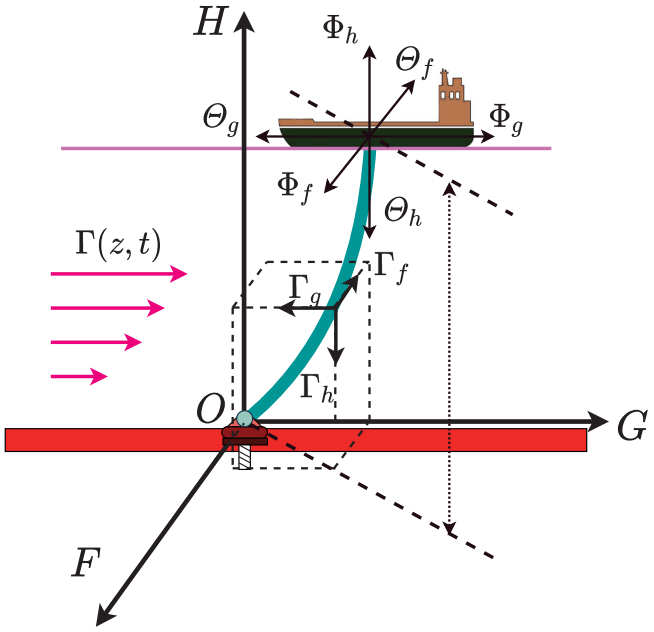

Fig. 1. Riser-vessel system.

$$m\ddot{g} = Tg' - EIg'''' + EA\left(h'g' + g''h'\right) + \frac{3}{2}EA\left(g'\right)^2 g'' + \frac{1}{2}EA\left[g''\left(f'\right)^2 + 2g'f'f''\right] + \Gamma_g, 0 < z < l \quad (2)$$

$$m\ddot{h} = EAh'' + EAf'f'' + EAg'g'' + \Gamma_h, 0 < z < l \quad (3)$$

$$f_0 = g_0 = h_0 = 0, f_0'' = g_0'' = h_0'' = 0,\ f_l'' = g_l'' = h_l'' = 0 \quad (4)$$

$$\omega_f\Phi_f + \Theta_f = M\ddot{f}_l + Tf_l' + \frac{1}{2}EA\left(f_l'\right)^3 + EAf_l'h_l' + \frac{1}{2}EAf_l'\left(g_l'\right)^2 - EIf_l'''' \quad (5)$$

$$\omega_g\Phi_g + \Theta_g = M\ddot{g}_l + Tg_l' + \frac{1}{2}EA\left(g_l'\right)^3 + EAg_l'h_l' + \frac{1}{2}EAg_l'\left(f_l'\right)^2 - EIg_l'''' \quad (6)$$

$$\omega_h\Phi_h + \Theta_h = M\ddot{h}_l + EAh_l' + \frac{1}{2}EA\left(f_l'\right)^2 + \frac{1}{2}EA\left(g_l'\right)^2 \quad (7)$$

where ω_i for $i = f, g, h$ denote unknown nonzero constants. The symbols EA, EI, m, T, and M symbolize axial stiffness bending stiffness, constant linear density, tension, and the mass of the vessel of the riser-vessel system, respectively.

B. Input Saturation and Input Quantization

The input saturation characteristic's model is proposed as [21]

$$u_i(u_{di}(t)) = \begin{cases} \text{sign}((u_{di}(t)))u_{Mi}, & \text{if } |u_{di}(t)| \geq u_{Mi} \\ u_{di}(t), & \text{if } |u_{di}(t)| < u_{Mi} \end{cases} \quad (8)$$

where u_{Mi}, $i = f, g, h$, are known positive constants and defined as the upper bounds of $u_i(u_{di}(t))$, $i = f, g, h$. We introduce a smooth function to approximate the saturation as [22]

$$u_i(u_{di}(t))) = h(u_{di}(t)) + d(u_{di}(t)) = u_{Mi} \times \tanh\frac{u_{di}(t)}{u_{Mi}} + d(u_{di}(t)) \quad (9)$$

where $d(u_{di}(t))$, $i = f, g, h$, can be regarded as the errors between $u_i(u_{di}(t))$ and $h(u_{di}(t))$, $i = f, g, h$.

According to the mean-value theorem, there exist constants μ_i with $0 < \mu_i < 1$, $i = f, g, h$, such that

$$h(u_{di}(t)) = h(u_{0i}) + h_{u_{\mu_i}}[u_{di}(t) - u_{0i}] \quad (10)$$

where $h_{u_{\mu_i}} = (\partial h(u_{di}(t))/\partial u_{di}(t))\,|_{u_{di}(t)=u_{\mu_i}}$, $u_{\mu_{di}} = \mu_{di}u_{di}(t) + (1-\mu_i)u_{0i}$. By choosing $u_{0i} = 0$, (10) can be written as

$$h(u_{di}(t)) = h_{u_{\mu_i}}u_{di}(t). \quad (11)$$

In quantization control, the common quantizers are hysteresis and logarithmic. In the present study, we opted for the hysteresis quantizer for controller design, primarily because it offers advantages in mitigating chattering while providing more accurate quantization levels. The hysteresis quantizer is elaborated in [16] as follows:

$$Q(u(t)) = \begin{cases} u_j\text{sgn}(u), & \text{if } \frac{u_j}{1+\delta} < |u| \leq u_j\dot{u} < 0, \text{ or } u_j < |u| \leq \frac{u_j}{1-\delta}, \dot{u} > 0 \\ u_j(1+\delta)\text{sgn}(u), & \text{if } u_j < |u| \leq \frac{u_j}{1-\delta}, \dot{u} < 0, \text{ or } \frac{u_j}{1-\delta} < |u| \leq \frac{u_j(1+\delta)}{1-\delta}, \dot{u} > 0 \\ 0, & \text{if } 0 \leq |u| < \frac{u_{\min}}{1+\delta}, \dot{u} < 0, \text{ or } \frac{u_{\min}}{1+\delta} \leq |u| < u_{\min}, \dot{u} > 0 \\ Q\left(u(t^-)\right), & \text{if } \dot{u} = 0 \end{cases} \quad (12)$$

where $u_j = \rho^{(1-j)}u_{\min}$ with $j = 1, 2, \ldots,$ and $\delta = ([1-\rho]/[1+\rho])$ with parameters $0 < \rho < 1$. $u_{\min}$ represents the dead-zone range for $Q(u(t))$, while the positive parameter ρ serves as a measure of quantization density, i.e., a smaller ρ corresponds to a coarser quantizer. $Q(u(t))$ is in the set $U = \{0, \pm u_j, \pm(1+\delta)u_j, j = 1, 2, \ldots\}$. $u(t)$ denotes the control command yet to be designed.

To address the complexities introduced by $Q(u_i(t))$, $i = f, g, h$, being quantized values, the hysteresis quantizer $Q(u_i(t))$, $i = f, g, h$, can be decomposed as follows:

$$Q(u_i(t)) = f(u_i(t))u_i(t) + g(u_i(t)) \quad (13)$$

where

$$f(u_i(t)) = \begin{cases} \frac{Q(u_i(t))}{u_i(t)}, & \text{if } Q(u_i(t)) \neq 0 \\ 1, & \text{if } Q(u_i(t)) = 0 \end{cases} \quad (14)$$

$$g(u_i(t)) = \begin{cases} 0, & \text{if } Q(u_i(t)) \neq 0 \\ -u_i(t), & \text{if } Q(u_i(t)) = 0. \end{cases} \quad (15)$$

Remark 1: The linear decomposition approach for the hysteresis quantizer was utilized in the controller design as presented in [23]. Contrasted with the linear decomposition, a novel nonlinear decomposition was first proposed in [24], and it is shown that there are some advantages in the development of the subsequent design scheme. More detailed discussions were made in [24]. Noted that, neither the quantizer parameter δ nor the dead-zone $u_{\min}$ can be predetermined when employing the nonlinear decomposition.

C. Actuator Fault

In practical engineering, actuators are susceptible to malfunctions, and the fault of the actuator pondered in this article can be characterized as follows [25]:

$$\Phi_i(t) = u_{hi}Q(u_i(t)) + u_{fi} \tag{16}$$

where u_{hi} and u_{fi}, $i = f, g, h$, denote the partial losses of effectiveness fault and float fault, respectively. When $u_{hi} = 0$, the actuators are stuck, rendering any controller ineffective. At $u_{hi} = 1$, the system operates normally without any faults. For values of $u_{hi} \in (0, 1)$, the system experiences a partial loss of effectiveness. This study focuses on control designs for scenarios where $u_{hi} \in (0, 1]$. In cases where $u_{hi} = 0$, implementing a redundant control strategy may be necessary to effectively address the issue [26].

D. Preliminaries

The subsequent design and analysis are facilitated by the introduction of the following assumptions and lemmas.

Assumption 1: For $\Theta_i(t), i = f, g, h$, we suppose that $\Lambda_i > 0, i = f, g, h$, such that $\mid \Theta_f(t) \mid \leq \Lambda_f$, $\mid \Theta_g(t) \mid \leq \Lambda_g$, and $\mid \Theta_h(t) \mid \leq \Lambda_h$. Suppose that there exist positive constants, $\bar{\Gamma}_f$, $\bar{\Gamma}_g$, and $\bar{\Gamma}_h$, satisfying $\mid \Gamma_f(z,t) \mid \leq \bar{\Gamma}_f$, $\mid \Gamma_g(z,t) \mid \leq \bar{\Gamma}_g$, and $\mid \Gamma_h(z,t) \mid \leq \bar{\Gamma}_h$, respectively. It is a reasonable assumption because disturbances possess finite energy [27].

Assumption 2: There exist unknown positive constants $\bar{u}_{fi}$ such that $\mid u_{fi} \mid \leq \bar{u}_{fi}$, $i = f, g, h$. It is a reasonable assumption because it usually arises from the natural limitations and design specifications of physical systems [28].

Lemma 1 [29]: Let $\beta_1(z,t)$ and $\beta_2(z,t)$ belongs to $\mathcal{R}$, defining $(z,t) \in [0,l] \times [0,+\infty)$, be derived as

$$\beta_1\beta_2 \leq \theta\beta_1^2 + \frac{1}{\theta}\beta_2^2 \tag{17}$$

where $\theta > 0$.

Lemma 2 [30]: Let $\beta(z,t) \in \mathcal{R}$, where $(z,t) \in [0,l] \times [0,+\infty)$. If it fulfills the condition $\beta(0,t) = 0$, the subsequent inequalities are valid

$$\beta^2 \leq l\int_0^l \beta'^2 dz \tag{18}$$

$$\int_0^l \beta^2 dz \leq l^2\int_0^l \beta'^2 dz. \tag{19}$$

Lemma 3 [16]: If p and r are scalars and satisfy $p \in \mathcal{R}, r \in \mathcal{R}^+$, we have

$$0 \leq \mid p \mid - \frac{p^2}{\sqrt{p^2 + r^2}} \leq r. \tag{20}$$

If $r > 0$ is an uniformly bounded continuous function with $\lim_{t\to\infty}\int_{t_0}^t r(\mu)d\mu \leq \bar{r}$, the above inequality is satisfied.

Lemma 4 [31]: Let $K(t)$ and $k(t)$ be smooth functions defined on the interval $[0, t_f)$ with $K(t) \geq 0$ for all t in $[0, t_f)$. Assume $K(t)$ is an even smooth Nussbaum-type function, and let θ_0 be a nonzero constant. If the subsequent inequality is satisfied

$$K(t) \leq \int_0^t (\theta_0 \nu(k(\tau)) + 1)\dot{k}(\tau)d\tau + C \tag{21}$$

where C represents a suitable constant, then $K(t), k(t)$, and $\int_0^t(\theta_0\nu(k(\tau)) - 1)\dot{k}(\tau)d\tau$ must be bounded on $[0, t_f)$. If θ_0 is a bounded function, the inequality still holds.

III. Control Design

Within this section, novel adaptive FTC strategies are formulated. These strategies aim to eliminate actuator faults, handle composite disturbances, suppress vibrations, and guarantee that the displacements remain within a predefined range.

To compensate for the unknown actuator faults, external disturbances, and quantization errors, we denote the composite disturbances $d_i(t)$, $i = f, g, h$, as follows:

$$d_i(t) = k_i u_{hi} f(u_i(t))d(u_{di}(t)) + k_i u_{hi} g(u_i(t)) + k_i u_{fi} + \Theta_i. \tag{22}$$

Invoking (22), (6) and (7) can be rewritten as

$$\begin{aligned} &M\ddot{f}_l + Tf_l' + \frac{1}{2}EA(f_l')^3 + EAf_l'h_l' + \frac{1}{2}EAf_l'(g_l')^2 \\ &\quad - EIf_l''' - d_f(t) - g_{ff}(u_f(t))u_{df}(t) = 0 \end{aligned} \tag{23}$$

$$\begin{aligned} &M\ddot{g}_l + Tg_l' + \frac{1}{2}EA(g_l')^3 + EAg_l'h_l' + \frac{1}{2}EAg_l'(f_l')^2 \\ &\quad - EIg_l''' - d_g(t) - g_{gf}(u_g(t))u_{dg}(t) = 0 \end{aligned} \tag{24}$$

$$\begin{aligned} &M\ddot{h}_l + EAh_l' + \frac{1}{2}EA(f_l')^2 + \frac{1}{2}EA(g_l')^2 - d_h(t) \\ &\quad - g_h f(u_h(t))u_{dh}(t) = 0 \end{aligned} \tag{25}$$

where $g_i = \omega_i u_{hi} h_{\mu_i}$ and $\underline{\lambda} = g_i(1-\delta) \leq g_i f(u_i) \leq g_i(1+\delta) = \bar{\lambda}$, $i = f, g, h$.

Then, we define the parameters D_i, $i = f, g, h$, as

$$\begin{aligned} D_i = \sup_{t\geq 0} &\mid \omega_i u_{hi} f(u_i(t))d(u_{di}(t)) + \omega_i u_{hi} g(u_i(t)) \mid \\ &+ \Lambda_i + \mid \omega_i \bar{u}_{fi} \mid . \end{aligned} \tag{26}$$

It is noteworthy to emphasize that the constants D_i for $i = f, g, h$ are both unknown and bounded, as per Assumptions 1 and 2. The values of D_i can be estimated through the subsequent design of a parameter adaptive law.

A. Adaptive FTC

The adaptive FTC laws are designed as

$$u_{df}(t) = -N_f(k_f)\Pi_f(t) \tag{27}$$

$$u_{dg}(t) = -N_g(k_g)\Pi_g(t) \tag{28}$$

$$u_{dh}(t) = -N_h(k_h)\Pi_h(t) \tag{29}$$

where Π_i, $i = f, g, h$, are presented as follows:

$$\begin{aligned} \Pi_f(t) = &M\beta l\dot{f}_l' + k_{f1}(\dot{f}_l + \beta l f_l') + 2k_{f2}(\dot{f}_l - \beta l f_l') \\ &+ \frac{(\dot{f}_l + \beta l f_l')\hat{D}_f^2}{\sqrt{(\dot{f}_l + \beta l f_l')^2\hat{D}_f^2 + \sigma^2(t)}} \end{aligned} \tag{30}$$

$$\begin{aligned} \Pi_g(t) = &M\beta l\dot{g}_l' + k_{g1}(\dot{g}_l + \beta l g_l') + 2k_{g2}(\dot{g}_l - \beta l g_l') \\ &+ \frac{(\dot{g}_l + \beta l g_l')\hat{D}_g^2}{\sqrt{(\dot{g}_l + \beta l g_l')^2\hat{D}_g^2 + \sigma^2(t)}} \end{aligned} \tag{31}$$

$$\begin{aligned} \Pi_h(t) = &M\beta l\dot{h}_l' + k_{h1}(\dot{h}_l + \beta l h_l') + 2k_{h2}(\dot{h}_l - \beta l h_l') \\ &+ \frac{(\dot{h}_l + \beta l h_l')\hat{D}_h^2}{\sqrt{(\dot{h}_l + \beta l h_l')^2\hat{D}_h^2 + \sigma^2(t)}} \end{aligned} \tag{32}$$

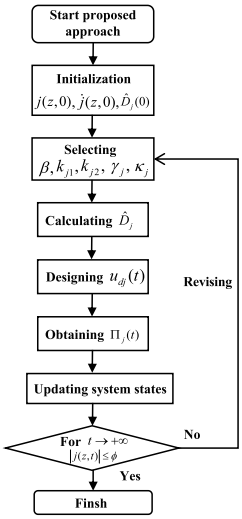

Fig. 2. Flowchart of the proposed approach (27)–(38) ($j = f, g, h$).

and $N_i(k_i) = e^{k_i^2}\cos([\pi/2]k_i)$, $i = f, g, h$, are the Nussbaum functions with k_i, $i = f, g, h$ generated by

$$\dot{k}_f(t) = \gamma_f\left(\dot{f}_l + \beta l f_l'\right)\Pi_f(t) \tag{33}$$

$$\dot{k}_g(t) = \gamma_g\left(\dot{g}_l + \beta l g_l'\right)\Pi_g(t) \tag{34}$$

$$\dot{k}_h(t) = \gamma_h\left(\dot{h}_l + \beta l h_l'\right)\Pi_h(t) \tag{35}$$

where β, k_{i1}, k_{i2}, and $\gamma_i > 0$, $i = f, g, h$. $\sigma(t)$ is uniformly bounded continuous functions with $\lim_{t\to\infty}\int_{t_0}^{t}\sigma(t)dt \le \bar{\sigma}$.

Now the adaptive laws are designed as

$$\dot{\hat{D}}_f = \kappa_f\left(\dot{f}_l + \beta l f_l'\right) - \kappa_f\sigma(t)\hat{D}_f \tag{36}$$

$$\dot{\hat{D}}_g = \kappa_g\left(\dot{g}_l + \beta l g_l'\right) - \kappa_g\sigma(t)\hat{D}_g \tag{37}$$

$$\dot{\hat{D}}_h = \kappa_h\left(\dot{h}_l + \beta l h_l'\right) - \kappa_h\sigma(t)\hat{D}_h \tag{38}$$

where κ_i, $i = f, g, h$ are positive constants. Fig. 2 shows the proposed design approach flowchart (27)–(38).

Remark 2: It will be shown that the term $[(\dot{l}_l + \beta l i_l')\hat{D}_i^2/\sqrt{(\dot{l}_l + \beta l i_l')^2\hat{D}_i^2 + \sigma^2(t)}]$ in (30)–(32) can be used to compensate for the effect of the external disturbance, the saturated compensation error, the error of the float fault, and the dead-zone for the quantizer is different from [32]. From (36)–(38), it is shown that $\sigma(t)$ − modification is used.

Remark 3: In the process of execution, we can obtain the signals $f_l, g_l, h_l, f_l', g_l', h_l', \dot{f}_l, \dot{g}_l, \dot{h}_l, \dot{f}_l', \dot{g}_l'$, and $\dot{h}_l'$ in the control laws (27)–(38) through sensors and corresponding algorithms. The signals f_l, g_l, and h_l can be measured by the laser displacement sensors and the signals f_l', g_l', and h_l' can be measured with inclinometers. In addition, the remaining signals $\dot{f}_l, \dot{g}_l, \dot{h}_l, \dot{f}_l', \dot{g}_l'$, and $\dot{h}_l'$ can be further obtained by the backward difference algorithm based on the measured values. In addition, hydraulic motors are generally used to generate control torque in practical industrial applications.

B. Stability Proof

A Lyapunov function $K(t)$ is designated as

$$K(t) = K_1(t) + K_2(t) + K_3(t) \tag{39}$$

where

$$K_1(t) = \frac{1}{2}\rho\int_0^l\left(\dot{f}^2 + \dot{g}^2 + \dot{h}^2\right)dz + \frac{1}{2}T\int_0^l\left(f'^2 + g'^2\right)dz + \frac{1}{2}EA\int_0^l\left(h' + \frac{1}{2}f'^2 + \frac{1}{2}g'^2\right)^2 dz + \frac{1}{2}EI\int_0^l\left(f''^2 + g''^2\right)dz \tag{40}$$

$$K_2(t) = \frac{1}{2}M\left(\dot{f}_l + \beta l f_l'\right)^2 + \frac{1}{2}M\left(\dot{g}_l + \beta l g_l'\right)^2 + \frac{1}{2\kappa_f}\tilde{D}_f^2 + \frac{1}{2}M\left(\dot{h}_l + \beta l h_l'\right)^2 + \frac{1}{2\kappa_g}\tilde{D}_g^2 + \frac{1}{2\kappa_h}\tilde{D}_h^2, \tag{41}$$

$$K_3(t) = \beta m\int_0^l z\left(\dot{f}f' + \dot{g}g' + \dot{h}h'\right)dz. \tag{42}$$

Lemma 5: The Lyapunov function given in (39) possesses both upper and lower bounds

$$0 \le \varkappa_1[G(t) + K_2(t)] \le K(t) \le \varkappa_2[G(t) + K_2(t)] \tag{43}$$

where $\varkappa_1, \varkappa_2 > 0$ and

$$G(t) \le \int_0^l(\dot{f}^2 + \dot{g}^2 + \dot{h}^2 + f'^2 + g'^2 + h'^2 + f'^4 + g'^4 + (f'g')2 + f''^2 + g''^2)dz. \tag{44}$$

Proof: See Appendix A. ■

Lemma 6: The $\dot{K}(t)$ is upper-bounded by

$$\dot{K}(t) \le -\varkappa K(t) + \zeta + \frac{1}{\gamma_f}\left(\Theta_f + 1\right)\dot{k}_f + \frac{1}{\gamma_g}\left(\Theta_g + 1\right)\dot{k}_g + \frac{1}{\gamma_h}(\Theta_h + 1)\dot{k}_h \tag{45}$$

where $\zeta, \varkappa$ are positive constants and $\Theta_i = g_i f(u_i)N_i(k_i)$, $i = f, g, h$.

Proof: See Appendix B. ■

Remark 4: According to the proof of Lemma 5, we can obtain appropriate parameters σ, β, and ϑ_1. Next, choosing appropriate parameters k_{f2}, k_{g2}, and k_{h2} satisfies (69)–(75). On this basis, we make the system converge by adjusting other parameters and then select a best set of parameters by trial and error.

Theorem 1: For the analyzed riser-vessel system described by (1)–(7), we implement the proposed adaptive FTC controllers along with the updating laws given in (27)–(38). Assuming the satisfaction of the specified constraints in (69)-(75) and bounded initial conditions, we can deduce that, by suitably choosing the parameters, the displacements of the riser-vessel system will converge to a narrow neighborhood around zero.

Proof: Through the multiplication of (45) by $e^{\varkappa t}$, we derive

$$K(t) \le K(0)e^{-\varkappa t} + \bar{\zeta} \tag{46}$$

where

$$\bar{\zeta} = \frac{\zeta}{\varkappa} + e^{-\varkappa t}\int_0^t\left(\frac{1}{\gamma_f}(\Theta_f + 1)\dot{k}_f\right)e^{\varkappa t}d\tau + e^{-\varkappa t}\int_0^t\left(\frac{1}{\gamma_g}(\Theta_g + 1)\dot{k}_g\right)e^{\varkappa t}d\tau + e^{-\varkappa t}\int_0^t\left(\frac{1}{\gamma_h}(\Theta_h + 1)\dot{k}_h\right)e^{\varkappa t}d\tau. \tag{47}$$

Utilizing $K_1(t)$, $G(t)$, and Lemma 2 yields

$$\frac{1}{l}f^2 \le \int_0^l f'^2dz \le G(t) \le \frac{1}{\varkappa_1}K(t) \le \frac{K(0)e^{-\varkappa t} + \bar{\zeta}}{\varkappa_1} \tag{48}$$

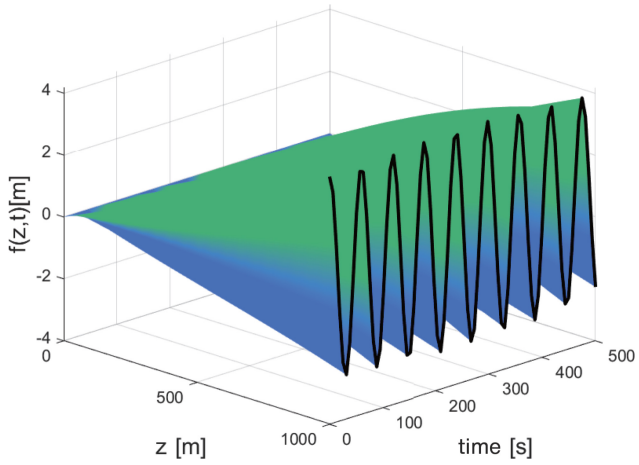

Fig. 3. $f(z,t)$ of the riser under no control.

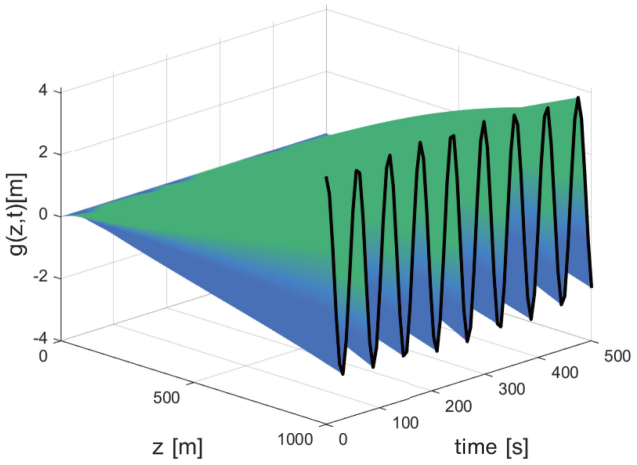

Fig. 4. $g(z,t)$ of the riser under no control.

$$\frac{1}{l}g^2 \le \int_0^l g'^2 dz \le G(t) \le \frac{1}{\varkappa_1}K(t) \le \frac{K(0)e^{-\varkappa t}+\bar{\zeta}}{\varkappa_1} \quad (49)$$

$$\frac{1}{l}h^2 \le \int_0^l h'^2 dz \le G(t) \le \frac{1}{\varkappa_1}K(t) \le \frac{K(0)e^{-\varkappa t}+\bar{\zeta}}{\varkappa_1}. \quad (50)$$

Substituting (48)–(50) into (46) obtains

$$|f(z,t)| \le \phi, |g(z,t)| \le \phi, |h(z,t)| \le \phi \quad (51)$$

with $\forall(z,t) \in [0,l] \times [0,+\infty)$ and $\phi = \sqrt{(l\bar{\zeta}/\varkappa_1\varkappa)}$. ■

IV. Numerical Simulation

To substantiate the efficacy of the proposed control scheme, numerical simulations are conducted employing the finite difference method. In this study, the simulation time step and spatial displacement are set to $\Delta t = 0.06$ s and $\Delta z = 50$ m, respectively. The simulation parameters employed in this study are detailed as follows: $f(z,0) = g(z,0) = h(z,0) = (4z/l)$, $EI = 1.22 \times 10^5$ Nm^2, $EA = 3.92 \times 10^7$ Nm^2, $c = 1.0$ Ns/m^2, $T = 2.75 \times 10^8$ N, $M = 9.6 \times 10^6$ kg, $m = 108$ kg/m, $l = 1000$ m, and $\dot{f}(z,0) = \dot{g}(z,0) = \dot{h}(z,0) = 0$. The parameters corresponding to the partial losses of effectiveness fault u_{ci} and float fault u_{fi} are 0.7 and 100, respectively. The form of unknown boundary disturbances on the vessel-riser system is given as $\Theta_f(t) = \Theta_g(t) = [1 + 5\sin(3t)] \times 10^5$ and $\Theta_h(t) = [2 + 2\sin(0.5t)] \times 10^5$. The disturbances $\Gamma_f(z,t)$, $\Gamma_g(z,t)$, and $\Gamma_h(z,t)$ are repressed as $\Gamma_f(z,t) = \Gamma_g(z,t) = (1/2)\rho_s C_D U^2(z,t)D + A_D \cos(4\pi f_q t + \alpha_0)$ and $\Gamma_h(z,t) = (1/2)\rho_s C_L U^2(z,t)D\cos(2\pi f_q t + \beta_0)$, where ρ_s, C_D, $U(z,t)$, D, A_D, f_q, and C_L denote the sea water density, drag coefficient, ocean surface current, external diameter of the riser, amplitude of the second term of $\Gamma_f(z,t)$ and $\Gamma_g(z,t)$ possessing 20% of the first term, vortex shedding frequency, and lift coefficient. α_0 and β_0 are the phase angles which are chosen to be 0. The values of these parameters are chosen with reference to [33].

Figs. 3–5 depict the responses of the riser-vessel system over both space and time in three dimensions in the absence of any control, i.e., with $\Phi_f = \Phi_g = \Phi_h = 0$. In the absence of control, the flexible riser experiences transverse deflections of up to 4 m. Prolonged and significant deflections result in irreversible damage to the riser. The parameters of the controller are provided in Table I, and the system responses

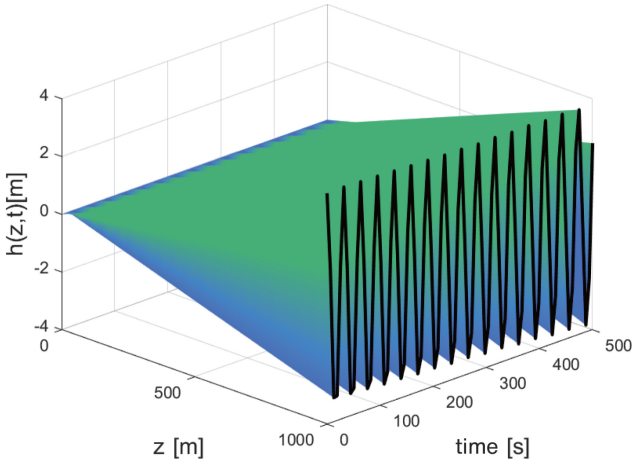

Fig. 5. $h(z,t)$ of the riser under no control.

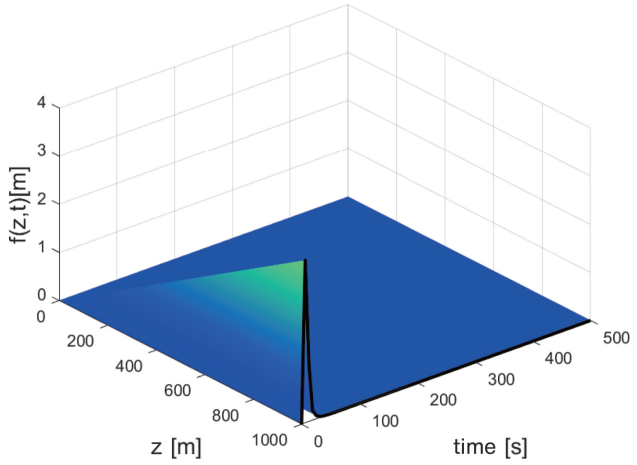

Fig. 6. $f(z,t)$ of the riser under the proposed control.

under these control settings are depicted in Figs. 6–8. These figures reveal that the proposed controllers are capable of effectively dampening vibrations even in external disturbances, unknown control direction, and the presence of actuator faults. When subject to the controllers, the deflection vibration of the riser is significantly suppressed within 100 s, which subsequently converges to zero after 150 s, and it demonstrates

TABLE I
CONTROL PARAMETERS

Param	Value	Param	Value	Param	Value
σ	0.25	β	4.9×10^{-4}	κ_i	1
k_{f1}	2	k_{f2}	5×10^7	γ_i	10^{-3}
k_{g1}	4	k_{g2}	1×10^7	$\sigma_i(t)$	$e^{-0.01t}$
k_{h1}	3	k_{h2}	6×10^7	$\bar{\sigma}$	0.25

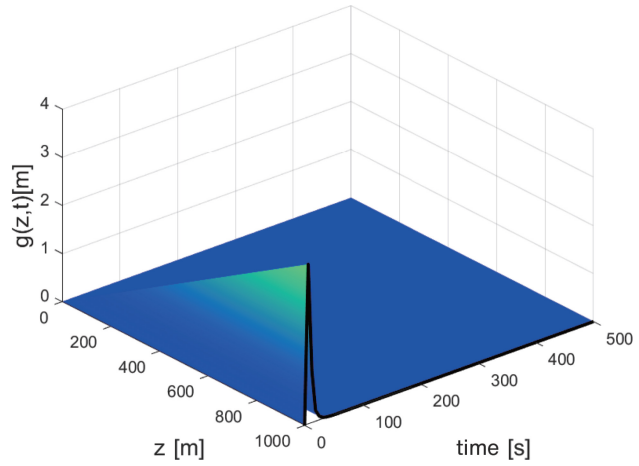

Fig. 7. $g(z, t)$ of the riser under the proposed control.

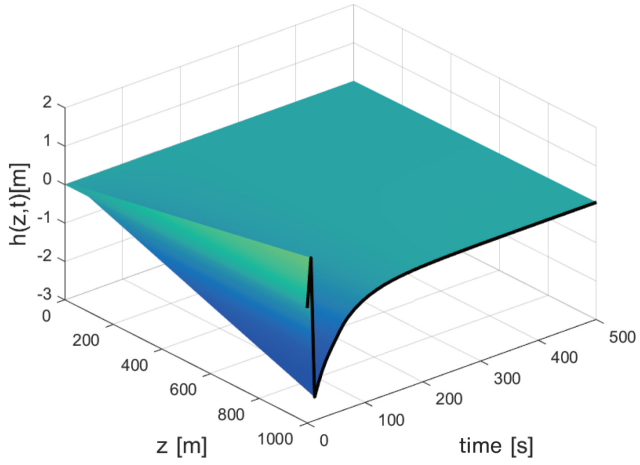

Fig. 8. $h(z, t)$ of the riser under the proposed control.

that a good control performance is ensured under the proposed control strategy. As illustrated in Figs. 9–11, the displacement amplitude at the top of the riser quickly converges. Similarly, the displacement amplitudes in all three directions converge to near zero within 150 s. Figs. 12–14 display the temporal responses of the actual control inputs. From the figures, we can infer that the proposed control inputs have been quantized, effectively reducing the communication frequency. Additionally, since the input saturation constraints of the actuators are considered, the proposed control signals remain within the specified limits, whereas the comparison control signals exceed these bounds. Moreover, it is evident that despite a 30% reduction in control inputs, the stability of the control system is effectively maintained. In conclusion, the formulated control strategies can contribute to stabilizing the riser-vessel system, markedly improving both its robustness and stability.

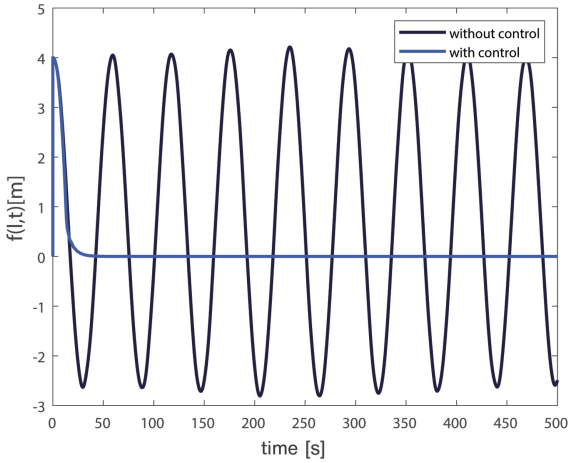

Fig. 9. $f(l, t)$ of the riser under the proposed control.

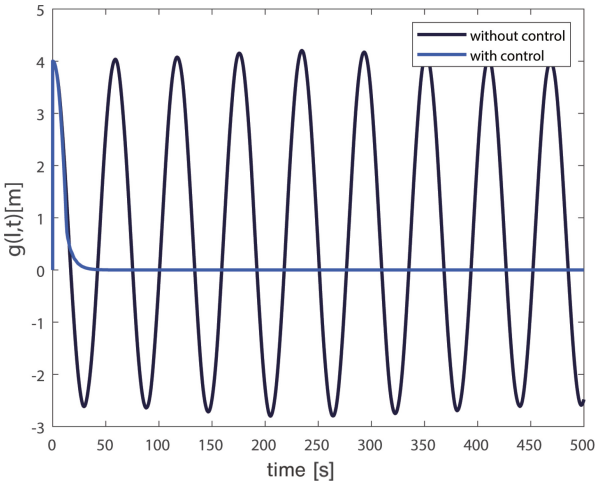

Fig. 10. $g(l, t)$ of the riser under the proposed control.

Remark 5: The simulation results shows that the proposed quantized control strategy can effectively address the control issues of 3-D riser-vessel system with unknown control direction, actuator faults, and input saturation, while also reducing the system's communication burden. However, this method has its limitations, as it cannot resolve control issues in the systems facing intermittent actuator faults. In the future, we plan to consider using neural network FTC to address this problem [34].

V. CONCLUSION

In this article, we developed a novel adaptive quantized FTC approach for a 3-D riser-vessel system, taking into account actuator faults, unknown control directions, and input saturation. Employing a bound estimation strategy, nonlinear decomposition for the quantizer, and a Nussbaum function, actuator faults, unknown control directions, input quantization, and external disturbances were effectively compensated. To tackle the issue of input saturation, control laws were formulated based on the HTO. The stability of the controlled system was rigorously established using the direct Lyapunov method. Numerical simulations, conducted via the finite difference method, corroborated the efficacy of the proposed strategy.

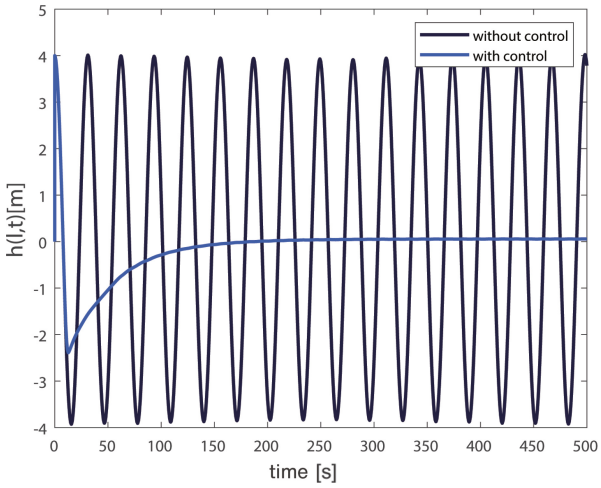

Fig. 11. $h(l,t)$ of the riser under the proposed control.

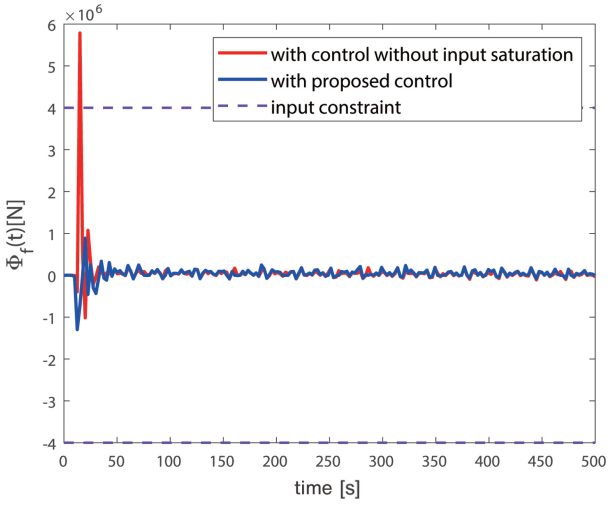

Fig. 12. Saturation quantization control input Φ_f.

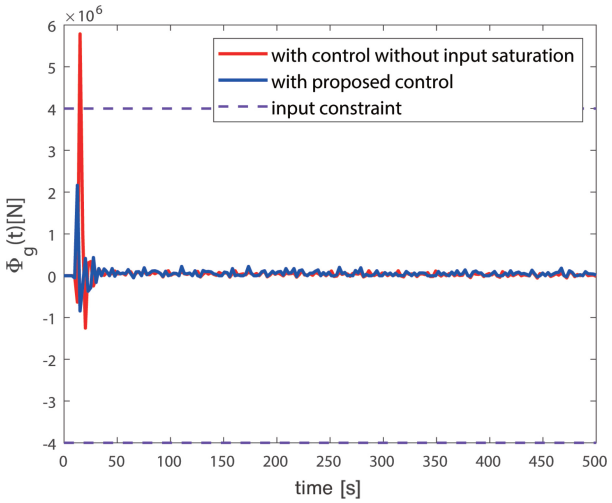

Fig. 13. Saturation quantization control input Φ_g.

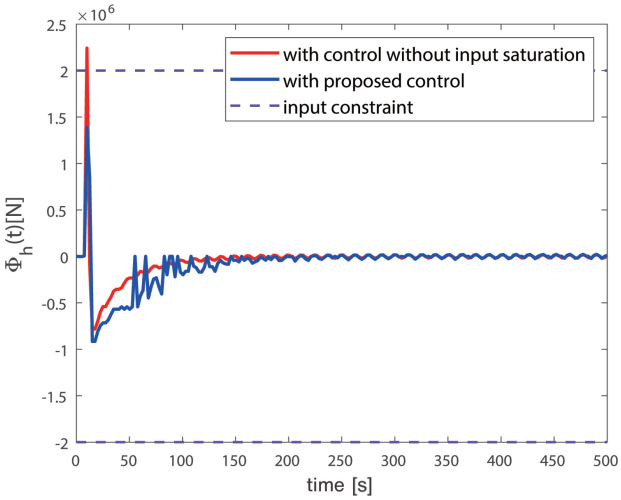

Fig. 14. Saturation quantization control input Φ_h.

The simulation results showed that the system states achieved uniformly bounded stability, and the control inputs in all three directions were maintained within the saturation limits, considering the input saturation constraints. Additionally, the system's inputs were quantized, effectively reducing the communication burden. The simulation results further demonstrated the effectiveness of the proposed control. However, there are some areas that need improvement. In the future, we intend to develop neural network control or reinforcement learning control strategy to handle system uncertainties and external disturbances [34], [35], [36], [37].

APPENDIX A
PROOF OF LEMMA 5

The expression for $K_1(t)$ can be reformulated as follows:

$$K_1(t) = \frac{1}{2}EA\int_0^l h'^2dz + \frac{1}{8}EA\int_0^l f'^4dz + \frac{1}{8}EA\int_0^l g'^4dz + \frac{1}{4}EA\int_0^l (f'g')2dz + \frac{1}{2}EI\int_0^l \left(f''^2 + g''^2\right)dz + \frac{1}{2}EA\int_0^l h'f'^2dz + \frac{1}{2}\rho\int_0^l \left(\dot{f}^2 + \dot{g}^2 + \dot{h}^2\right)dz + \frac{1}{2}EA\int_0^l h'g'^2dz + \frac{1}{2}T\int_0^l \left(f'^2 + g'^2\right)dz. \quad (52)$$

Invoking $(f_l')^2 \geq 2(h'l)^2$, and $(g_l')^2 \geq 2(h'l)^2$ gives

$$-\sigma\int_0^l f'^4dz - \frac{1}{2\sigma}\int_0^l f'^2dz \leq \int_0^l h'f'^2dz \leq \sigma\int_0^l f'^4dz + \frac{1}{2\sigma}\int_0^l f'^2dz \quad (53)$$

$$-\sigma\int_0^l g'^4dz - \frac{1}{2\sigma}\int_0^l g'^2dz \leq \int_0^l h'g'^2dz \leq \sigma\int_0^l g'^4dz + \frac{1}{2\sigma}\int_0^l g'^2dz \quad (54)$$

where σ is a positive constant.

By selecting an appropriate parameter σ to meet the conditions $T - (EA/2\sigma) \geq 0$ and $0 < \sigma \leq (1/4)$, we obtain

$$0 \leq \vartheta_1 G(t) \leq K_1(t) \leq \vartheta_2 G(t) \quad (55)$$

where

$$\vartheta_1 = \frac{1}{2}\min\left[\frac{1}{2}\mathrm{EA}, \mathrm{EA}\left(\frac{1}{4}-\sigma\right), \mathrm{T}-\frac{\mathrm{EA}}{2\sigma}, \mathrm{EI}, \mathrm{m}\right] \quad (56)$$

$$\vartheta_2 = \frac{1}{2}\max\left[\frac{1}{2}\mathrm{EA}, \mathrm{EA}\left(\frac{1}{4}+\sigma\right), \mathrm{T}+\frac{\mathrm{EA}}{2\sigma}, \mathrm{EI}, \mathrm{m}\right]. \quad (57)$$

The following can be deduced from Lemma 1:

$$|K_3(t)| \le \beta ml \int_0^l \left(\dot{f}^2+\dot{g}^2+\dot{h}^2+f'^2+g'^2+h'^2\right)dz \le \kappa_1 G(t) \quad (58)$$

where $\kappa_1 = \beta ml > 0$. Invoking (58) yields $-\kappa_1 G(t) \le K_3(t) \le \kappa_1 G(t)$. If β satisfies $0 < \beta < \vartheta_1/(ml)$, we obtain $0 < \kappa_1 < \vartheta_1$

$$0 \le \kappa_2 G(t) \le K_1(t) + K_3(t) \le \kappa_3 G(t) \quad (59)$$

where $\kappa_2 = \vartheta_1 - \kappa_1$ and $\kappa_3 = \vartheta_2 + \kappa_1$.

Examining $K_2(t)$, if we carefully choose values for $\varkappa_1$ and $\varkappa_2$ to satisfy $\varkappa_1 = \min(\kappa_2, 1) > 0$ and $\varkappa_2 = \max(\kappa_3, 1) > 0$, we can establish Lemma 4 as follows:

$$0 \le \varkappa_1(G(t)+K_2(t)) \le K(t) \le \varkappa_2(G(t)+K_2(t)). \quad (60)$$

This completes the proof.

Appendix B
Proof of Lemma 6

The $\dot{K}(t)$ is

$$\dot{K}(t) = \dot{K}_1(t) + \dot{K}_2(t) + \dot{K}_3(t). \quad (61)$$

The expression for $\dot{K}_1(t)$ can be derived as

$$\begin{aligned}
\dot{K}_1(t) &= m\int_0^l (\dddot{f}f + \ddot{g}\ddot{g} + \dot{h}\ddot{h})dz \\
&\quad + EA\int_0^l \left[\left(h' + \frac{1}{2}(f')^2 + \frac{1}{2}(g')^2\right)(\dot{h}' + \dot{f}'f' + \dot{g}'g')\right]dz \\
&\quad + EI\int_0^l (f''\dddot{f}'' + g''\dddot{g}'')dz + T\int_0^l (f'\dddot{f}' + g'\dddot{g}')dz \\
&= \int_0^l \dot{f}[Tf'' + EA(h''f' + f''h') + \frac{3}{2}EA(f')^2 f'' \\
&\quad + \frac{1}{2}EA[f'(f')2 + 2f'g'g'] - EIf'' + d_f]dz \\
&\quad + \int_0^l \dot{g}[Tg' + EA(h'g' + g''h') + \frac{3}{2}EA(g')^2 g'' \\
&\quad + \frac{1}{2}EA[g'(f')^2 + 2g'ff'] - EIg'''' + d_g]dz \\
&\quad + \int_0^l \dot{h}[EAh'' + EAf'f'' + EAg'g'' + d_h]dz \\
&\quad + EAh'_l\dot{h}_l - EA\int_0^l h''\dot{h}dz + EAh'_lg'_l\dot{f}_l \\
&\quad - EA\int_0^l (f''g' + f'g'')\dot{f}dz + EAg'_lh'_l\dot{h}_l \\
&\quad - EA\int_0^l (h''g' + h'g'')\dot{g}dz + \frac{1}{2}EA(g'_l)^2\dot{h}_l \\
&\quad - EA\int_0^l g'g''\dot{h}dz + \frac{1}{2}EA(g'_l)^3\dot{g}_l \\
&\quad - EA\int_0^l f'f''\dot{h}dz - \frac{3}{2}EA\int_0^l (g')^2 g''\dot{g}dz \\
&\quad + \frac{1}{2}EA(g'_l)^2 f'_l\dot{f}_l + \frac{1}{2}EA(f'_l)^2 g'_l\dot{g} \\
&\quad - \frac{1}{2}EA\int_0^l (2f'f''g' + f'^2g'')\dot{g}dz \\
&\quad - \frac{1}{2}EA\int_0^l (2g'g''f' + g'^2f'')\dot{f}dz \\
&\quad + \frac{1}{2}EA(f'_l)^3\dot{f}_l - \frac{3}{2}EA\int_0^l (f')^2 f''\dot{f}dz - EIf'_l\dot{f}_l \\
&\quad + EI\int_0^l f'\dot{f}dz - EIg''''_l\dot{g}_l + EI\int_0^l g''\dot{g}dz \\
&\quad + T(f'_l\dot{f}_l + g'_l\dot{g}_l) - T\int_0^l (f''\dot{f} + g''\dot{g})dz \\
&= \int_0^l [\dot{f}\Gamma_f + \dot{g}\Gamma_g + \dot{h}\Gamma_h]dz + \Xi_f\dot{f}_l + \Xi_g\dot{g}_l + \Xi_h\dot{h}_l \quad (62)
\end{aligned}$$

where

$$\Xi_f = Tf'_l + \frac{1}{2}EA(f'_l)^3 + EAf'_lh'_l + \frac{1}{2}EAf'_l(g'_l)^2 - EIf'''_l \quad (63)$$

$$\Xi_g = Tg'_l + \frac{1}{2}EA(g'_l)^3 + EAg'_lh'_l + \frac{1}{2}EAg'_l(f'_l)^2 - EIg'''_l \quad (64)$$

$$\Xi_h = EAh'_l + \frac{1}{2}EA(f'_l)^2 + \frac{1}{2}EA(g'_l)^2. \quad (65)$$

Moreover, $\dot{K}_2(t)$ is obtained as

$$\begin{aligned}
\dot{K}_2(t) &= M(\dot{f}_l + \beta lf'_l)(\ddot{f}_l + \beta l\dot{f}'_l) + M(\dot{g}_l + \beta lg'_l)(\ddot{g}_l + \beta l\dot{g}'_l) \\
&\quad + M(\dot{h}_l + \beta lh'_l)(\ddot{h}_l + \beta l\dot{h}'_l) - \frac{1}{\kappa_f}\tilde{D}_f\dot{\tilde{D}}_f - \frac{1}{\kappa_g}\tilde{D}_g\dot{\tilde{D}}_g \\
&\quad - \frac{1}{\kappa_h}\tilde{D}_h\dot{\tilde{D}}_h. \quad (66)
\end{aligned}$$

Furthermore, the $\dot{K}_3(t)$ is obtained as

$$\begin{aligned}
\dot{K}_3(t) &= \beta m\int_0^l z(\dddot{f}f' + \ddot{f}\dot{f}' + \ddot{g}g' + \dot{g}\dot{g}' + \ddot{h}h' + \dot{h}\dot{h}')dz \\
&= -\frac{3}{8}\beta EA\int_0^l f'^4dz - \frac{3}{8}\beta EA\int_0^l g'^4dz \\
&\quad - \beta EA\int_0^l h'f'^2dz - \beta EA\int_0^l h'g'^2dz \\
&\quad - \frac{3}{4}\beta EA\int_0^l (f'g')^2dz - \frac{3}{2}\beta EI\int_0^l f''^2dz \\
&\quad - \frac{3}{2}\beta EI\int_0^l g''^2dz - \frac{1}{2}\beta T\int_0^l f'^2dz \\
&\quad - \frac{1}{2}\beta T\int_0^l g'^2dz - \frac{1}{2}\beta EAl\left[\frac{1}{2}(f'_l)^2 + \frac{1}{2}(g'_l)^2 + (h'_l)\right]^2 \\
&\quad - \frac{1}{2}\beta Tl(f'_l)^2 - \frac{1}{2}\beta Tl(g'_l)^2 - \frac{1}{2}\beta EA\int_0^l h'^2dz \\
&\quad - \frac{1}{2}\beta m\int_0^l \dot{f}^2dz - \frac{1}{2}\beta m\int_0^l \dot{g}^2dz - \frac{1}{2}\beta m\int_0^l \dot{h}^2dz \\
&\quad + \frac{1}{2}\beta ml\left[(\dot{f}_l)^2 + (\dot{g}_l)^2 + (\dot{h}_l)^2\right] \\
&\quad + \beta lf'_l\Xi_f + \beta lg'_l\Xi_g + \beta lh'_l\Xi_h \\
&\quad + \beta\int_0^l z(f'd_f + g'd_g + h'd_h)dz. \quad (67)
\end{aligned}$$

Invoking $(f_l')^2 \geq 2(h_l')^2$, $(g_l')^2 \geq 2(h_l')^2$, and Lemmas 2–3, the differentiation of $K(t)$ and substitution of the control laws (27)–(38) yields

$$\begin{aligned}\dot{K}(t) \leq & -\left(\frac{1}{2}\beta m-\frac{1}{\iota_1}\right)\int_0^l \dot{f}^2dz-\left(\frac{3}{8}\beta EA-\frac{\beta EA}{2\iota_7}\right)\int_0^l f'^4dz\\ & -\left(\frac{1}{2}\beta m-\frac{1}{\iota_2}\right)\int_0^l \dot{g}^2dz-\left(\frac{3}{8}\beta EA-\frac{\beta EA}{2\iota_8}\right)\int_0^l g'^4dz\\ & -\left(\frac{1}{2}\beta m-\frac{1}{\iota_3}\right)\int_0^l \dot{h}^2dz-\left(\frac{1}{2}\beta EA-\beta l\iota_6\right)\int_0^l h'^2dz\\ & -\left(\frac{1}{2}\beta T-\beta l\iota_4-\frac{\beta EA\iota_7}{4}\right)\int_0^l f'^2dz\\ & -\left(\frac{1}{2}\beta T-\beta l\iota_5-\frac{\beta EA\iota_8}{4}\right)\int_0^l g'^2dz\\ & +\left(\iota_1+\frac{\beta l}{\iota_4}\right)\int_0^l \bar{\Gamma}_f^2dz+\left(\iota_2+\frac{\beta l}{\iota_5}\right)\int_0^l \bar{\Gamma}_g^2dz\\ & +\left(\iota_3+\frac{\beta l}{\iota_6}\right)\int_0^l \bar{\Gamma}_h^2dz-\left(k_{f2}-\frac{1}{2}\beta ml\right)\dot{f}_l^2\\ & -\left(k_{g2}-\frac{1}{2}\beta ml\right)\dot{g}_l^2-\left(k_{h2}-\frac{1}{2}\beta ml\right)\dot{h}_l^2\\ & -\frac{3}{2}\beta EI\int_0^l f''^2dz-\frac{3}{2}\beta EI\int_0^l g''^2dz\\ & -\frac{1}{2}\beta EAl\left[\frac{1}{2}(f_l')^2+\frac{1}{2}(g_l')^2+h_l'\right]^2\\ & -\left(\frac{1}{4}\beta Tl-k_{f2}\beta^2l^2\right)(f_l')^2-\left(\frac{1}{4}\beta Tl-k_{g2}\beta^2l^2\right)(g_l')^2\\ & -\left(\beta Tl-k_{h2}\beta^2l^2\right)(h_l')^2-\frac{3}{4}\beta EA\int_0^l (f'g')^2dz\\ & +\frac{1}{\gamma_f}\left(g_ff(u_f)N_f(k_f)+1\right)\dot{k}_f+\frac{\bar{\sigma}}{2}D_f^2-\frac{\bar{\sigma}}{2}\tilde{D}_f^2\\ & +\frac{1}{\gamma_g}\left(g_gf(u_g)N_g(k_g)+1\right)\dot{k}_g+\frac{\bar{\sigma}}{2}D_g^2-\frac{\bar{\sigma}}{2}\tilde{D}_g^2\\ & +\frac{1}{\gamma_h}\left(g_hf(u_h)N_h(k_h)+1\right)\dot{k}_h+\frac{\bar{\sigma}}{2}D_h^2-\frac{\bar{\sigma}}{2}\tilde{D}_h^2+3\bar{\sigma} \end{aligned} \tag{68}$$

where $\iota_1 \sim \iota_8 > 0$, and the parameters β, k_{f2}, k_{g2}, and k_{h2}, are chosen to satisfy

$$\nu_1=\frac{1}{2}\beta m-\frac{1}{\iota_1}>0,\quad \nu_2=\frac{1}{2}\beta m-\frac{1}{\iota_2}>0 \tag{69}$$

$$\nu_3=\frac{1}{2}\beta m-\frac{1}{\iota_3}>0,\quad \nu_4=\frac{1}{2}T-l\iota_4-\frac{EA\iota_7}{4}>0 \tag{70}$$

$$\nu_5=\frac{1}{2}T-l\iota_5-\frac{EA\iota_8}{4}>0,\quad \nu_6=\frac{1}{2}EA-l\iota_6>0 \tag{71}$$

$$\nu_7=\frac{3}{8}EA-\frac{EA}{2\iota_7}>0,\quad \nu_8=\frac{3}{8}EA-\frac{EA}{2\iota_8}>0 \tag{72}$$

$$T-4k_{f2}\beta l\geq 0,\quad T-4k_{g2}\beta l\geq 0,\quad T-k_{h2}\beta l\geq 0 \tag{73}$$

$$k_{f2}-\frac{1}{2}\beta ml\geq 0,\quad k_{g2}-\frac{1}{2}\beta ml\geq 0,\quad k_{h2}-\frac{1}{2}\beta ml\geq 0 \tag{74}$$

$$\zeta=\left(\iota_1+\frac{\beta l}{\iota_4}\right)\bar{\Gamma}_f^2+\left(\iota_2+\frac{\beta l}{\iota_5}\right)\bar{\Gamma}_g^2+\left(\iota_3+\frac{\beta l}{\iota_6}\right)\bar{\Gamma}_h^2+\frac{\bar{\sigma}}{2}\left(D_f^2+D_g^2+D_h^2\right)+3\bar{\sigma}<+\infty. \tag{75}$$

Invoking (75)–(75) and Lemma 4, we obtain

$$\begin{aligned}\dot{K}(t)\leq & -\nu_1\int_0^l \dot{f}^2dz-\nu_2\int_0^l \dot{g}^2dz-\nu_3\int_0^l \dot{h}^2dz\\ & -\nu_4\int_0^l f'^2dz-\nu_5\int_0^l g'^2dz-\nu_6\int_0^l h'^2dz\\ & -\nu_7\int_0^l f'^4dz-\nu_8\int_0^l g'^4dz-\frac{3}{2}\beta EI\int_0^l f''^2dz\\ & -\frac{3}{2}\beta EI\int_0^l g''^2dz-\frac{3}{4}\beta EA\int_0^l (f'g')^2dz\\ & -\frac{\bar{\sigma}}{2}\left(\tilde{D}_f^2+\tilde{D}_g^2+\tilde{D}_h^2\right)+\zeta+\frac{1}{\gamma_f}(\Theta_f+1)\dot{k}_f\\ & +\frac{1}{\gamma_g}(\Theta_g+1)\dot{k}_g+\frac{1}{\gamma_h}(\Theta_h+1)\dot{k}_h\\ \leq & -\varkappa_3(G(t)+K_2(t))+\zeta+\frac{1}{\gamma_f}(\Theta_f+1)\dot{k}_f\\ & +\frac{1}{\gamma_g}(\Theta_g+1)\dot{k}_g+\frac{1}{\gamma_h}(\Theta_h+1)\dot{k}_h \end{aligned} \tag{76}$$

where $\varkappa_3 = \min(\nu_1, \nu_2, \nu_3, \nu_4, \nu_5, \nu_6, \nu_7, \nu_8, (3/2)\beta EI, (3/4)\beta EA, (k_{f1}/M), [k_{g1}/M], [k_{h1}/M])$. Therefore, invoking Lemma 4 and (76), we get

$$\begin{aligned}\dot{K}(t)\leq & -\varkappa K(t)+\zeta+\frac{1}{\gamma_f}(\Theta_f+1)\dot{k}_f\\ & +\frac{1}{\gamma_g}(\Theta_g+1)\dot{k}_g+\frac{1}{\gamma_h}(\Theta_h+1)\dot{k}_h \end{aligned} \tag{77}$$

where $\varkappa=(\varkappa_3/\varkappa_2)$.

This completes the proof.

REFERENCES

[1] K. D. Do, "Inverse optimal gain assignment control of evolution systems and its application to boundary control of marine risers," *Automatica*, vol. 106, pp. 242–256, Aug. 2019.

[2] C. Yu, H. Lin, X. Lou, and J. Jia, "Boundary control of a flexible beam with output constraint under saturation input," *Int. J. Model., Identif. Control*, vol. 42, no. 2, pp. 116–130, 2023.

[3] W. He and S. S. Ge, "Vibration control of a flexible string with both boundary input and output constraints," *IEEE Trans. Control Syst. Technol.*, vol. 23, no. 4, pp. 1245–1254, Jul. 2015.

[4] W. He, X. Tang, T. Wang, and Z. Liu, "Trajectory tracking control for a three-dimensional flexible wing," *IEEE Trans. Control Syst. Technol.*, vol. 30, no. 5, pp. 2243–2250, Sep. 2022.

[5] S. Zhang, Q. Li, X. Zhao, Z. Liu, and G. Li, "Vibration control for an active mass damper of a high-rise building with input and output constraints," *IEEE/ASME Trans. Mechatronics*, vol. 28, no. 1, pp. 186–196, Feb. 2023.

[6] S. Zhang, X. Qian, Z. Liu, Q. Li, and G. Li, "PDE modeling and tracking control for the flexible tail of an autonomous robotic fish," *IEEE Trans. Syst., Man, Cybern., Syst.*, vol. 52, no. 12, pp. 7618–7627, Dec. 2022.

[7] Y. Liu, X. Chen, Y. Mei, and Y. Wu, "Observer-based boundary control for an asymmetric output-constrained flexible robotic manipulator," *Sci. China. Inf. Sci.*, vol. 65, no. 3, 2022, Art. no. 139203.

[8] K. Shao, J. Zheng, R. Tang, X. Li, Z. Man, and B. Liang, "Barrier function-based adaptive sliding mode control for uncertain systems with input saturation," *IEEE/ASME Trans. Mechatronics*, vol. 27, no. 6, pp. 4258–4268, Dec. 2022.

[9] Y. Hu, H. Yan, H. Zhang, M. Wang, and L. Zeng, "Robust adaptive fixed-time sliding-mode control for uncertain robotic systems with input saturation," *IEEE Trans. Cybern.*, vol. 53, no. 4, pp. 2636–2646, Apr. 2023.

[10] Z. Cao, L. Zhang, B. Niu, G. Zong, and X. Zhao, "Observer-based adaptive output-constrained control design of switched stochastic nonlinear systems with input saturation," *Asian J. Control*, vol. 25, no. 4, pp. 2961–2974, 2023.

[11] Y. Liu, F. Guo, X. He, and Q. Hui, "Boundary control for an axially moving system with input restriction based on disturbance observers," *IEEE Trans. Syst., Man, Cybern., Syst.*, vol. 49, no. 11, pp. 2242–2253, Nov. 2019.

[12] Y. Liu, X. Yao, and W. Zhao, "Distributed neural-based fault-tolerant control of multiple flexible manipulators with input saturations," *Automatica*, vol. 156, Oct. 2023, Art. no. 111202.

[13] W. Shi, M. Hou, and G. Duan, "Prescribed-time asymptotic tracking control of strict feedback systems with time-varying parameters and unknown control direction," *IEEE Trans. Circuits Syst. I, Reg. Papers*, vol. 69, no. 12, pp. 5259–5272, Dec. 2022.
[14] H. Wang, X. Zhou, and Y. Tian, "Robust adaptive fault-tolerant control using RBF-based neural network for a rigid-flexible robotic system with unknown control direction," *Int. J. Robust Nonlinear Control*, vol. 32, no. 3, pp. 1272–1302, 2022.
[15] J. Yu, P. Shi, C. Lin, and H. Yu, "Adaptive neural command filtering control for nonlinear MIMO systems with saturation input and unknown control direction," *IEEE Trans. Cybern.*, vol. 50, no. 6, pp. 2536–2545, Jun. 2019.
[16] Z. Zhao et al., "Adaptive quantized control of flexible manipulators subject to unknown dead zones," *IEEE Trans. Syst., Man, Cybern., Syst.*, vol. 53, no. 10, pp. 6438–6447, Oct. 2023.
[17] X. Yang, G. Feng, C. He, and J. Cao, "Event-triggered dynamic output Quantization control of switched T–S fuzzy systems with unstable modes," *IEEE Trans. Fuzzy Syst.*, vol. 30, no. 10, pp. 4201–4210, Oct. 2022.
[18] Z. Zhang, C. Wen, L. Xing, and Y. Song, "Adaptive output feedback control of nonlinear systems with mismatched uncertainties under input/output quantization," *IEEE Trans. Autom. Control*, vol. 67, no. 9, pp. 4801–4808, Sep. 2022.
[19] R. Zhao, Z. Zuo, and Y. Wang, "Event-triggered control for networked switched systems with quantization," *IEEE Trans. Syst., Man, Cybern., Syst.*, vol. 52, no. 10, pp. 6120–6128, Oct. 2022.
[20] Z. Zhao, Y. Liu, T. Zou, and K.-S. Hong, "Robust adaptive control of a riser-vessel system in three-dimensional space," *IEEE Trans. Syst., Man, Cybern., Syst.*, vol. 52, no. 7, pp. 4447–4456, Jul. 2022.
[21] L. Li, Z. Liu, S. Guo, Z. Ma, and P. Huang, "Adaptive practical predefined-time control for uncertain teleoperation systems with input saturation and output error constraints," *IEEE Trans. Ind. Electron.*, vol. 71, no. 2, pp. 1842–1852, Feb. 2024.
[22] T. Zhang, D. Yu, K. H. Cheong, Y. Zhao, Z. Wang, and C. L. P. Chen, "Nonsingular practical fixed-time consensus tracking for multimotor system with input saturation," *IEEE Syst. J.*, vol. 17, no. 3, pp. 4683–4694, Sep. 2023.
[23] J. Zhou, C. Wen, and G. Yang, "Adaptive backstepping stabilization of nonlinear uncertain systems with quantized input signal," *IEEE Trans. Autom. Control*, vol. 59, no. 2, pp. 460–464, Feb. 2014.
[24] G. Lai, Z. Liu, C. P. Chen, and Y. Zhang, "Adaptive asymptotic tracking control of uncertain nonlinear system with input quantization," *Syst. Control Lett.*, vol. 96, pp. 23–29, Oct. 2016.
[25] X. Wang, Y. Zhou, T. Huang, and P. Chakrabarti, "Event-triggered adaptive fault-tolerant control for a class of nonlinear multiagent systems with sensor and actuator faults," *IEEE Trans. Circuits Syst. I, Reg. Papers*, vol. 69, no. 10, pp. 4203–4214, Oct. 2022.
[26] S. Gao and J. Liu, "Adaptive fault-tolerant vibration control of a wind turbine blade with actuator stuck," *Int. J. Control*, vol. 93, no. 3, pp. 713–724, 2020.
[27] Q. Yao, Q. Li, Y. Xi, and H. Jahanshahi, "Extended state filter-based velocity-free finite-time attitude control of spacecraft," *Int. J. Robust Nonlinear Control*, vol. 34, no. 8, pp. 5540–5552, 2024.
[28] Q. Shen, P. Shi, and C. P. Lim, "Fuzzy adaptive fault-tolerant stability control against novel actuator faults and its application to mechanical systems," *IEEE Trans. Fuzzy Syst.*, vol. 32, no. 4, pp. 2331–2340, Apr. 2024.
[29] X. Yao, H. Sun, Z. Zhao, and Y. Liu, "Event-triggered bipartite consensus tracking and vibration control of flexible Timoshenko manipulators under time-varying actuator faults," *IEEE/CAA J. of Automatica Sinica*, vol. 11, no. 5, pp. 1190–1201, May 2024.
[30] Z. Liu, J. Shi, Y. He, Z. Zhao, and H.-K. Lam, "Adaptive fuzzy control for a spatial flexible hose system with dynamic event-triggered mechanism," *IEEE Trans. Aerosp. Electron. Syst.*, vol. 59, no. 2, pp. 1156–1167, Apr. 2023.
[31] Y.-H. Jing and G.-H. Yang, "Adaptive quantised fault-tolerant tracking control of uncertain nonlinear systems with unknown control direction and the prescribed accuracy," *Int. J. Syst. Sci.*, vol. 48, no. 13, pp. 2826–2837, 2017.
[32] C. Wang, C. Wen, and Y. Lin, "Adaptive actuator failure compensation for a class of nonlinear systems with unknown control direction," *IEEE Trans. Autom. Control*, vol. 62, no. 1, pp. 385–392, Jan. 2017.
[33] W. He, S. S. Ge, B. V. E. How, and Y. S. Choo, *Dynamics and Control of Mechanical Systems in Offshore Engineering*. London, U.K.: Springer, 2014.
[34] Y. Ma, X. He, S. Zhang, Y. Sun, and Q. Fu, "Adaptive compensation for infinite number of actuator faults and time-varying delay of a flexible manipulator system," *IEEE Trans. Ind. Electron.*, vol. 69, no. 12, pp. 13141–13150, Dec. 2022.
[35] Y. Lian, J. Xia, J. H. Park, W. Sun, and H. Shen, "Disturbance observer-based adaptive neural network output feedback control for uncertain nonlinear systems," *IEEE Trans. Neural Netw. Learn. Syst.*, vol. 34, no. 10, pp. 7260–7270, Oct. 2023.
[36] T. Li, G. Zhang, T. Zhang, and J. Pan, "Adaptive neural network tracking control of robotic manipulators based on disturbance observer," *Processes*, vol. 12, no. 3, p. 499, 2024.
[37] G. Li, X. Ma, and Y. Li, "Robust command shaped vibration control for stacker crane subject to parameter uncertainties and external disturbances," *IEEE Trans. Ind. Electron.*, vol. 71, no. 11, pp. 14740–14752, Nov. 2024.

Xiaowei Wang received the M.S. and Ph.D. degrees in electric machinery and electrical appliances from the Institute of Electrical Engineering, Harbin Institute of Technology, Harbin, China, in 2006 and 2014, respectively.

He entered Postdoctoral Workstation with the Shenzhen Academy of Aerospace Technology, Shenzhen, China, from 2014 to 2016. He is currently a Lecturer with the School of Mechanical and Electrical Engineering, Guangzhou University, Guangzhou, China. His research interests include electric machine, power electronics, and control systems.

Baoshan Zhang received the B.Sc. degree in electronic information engineering from the University of Electronic Science and Technology of China, Chengdu, China, in 2020.

He currently serves as the Product Manager for Henan Nengchuang Electronic Technology Company Ltd., Guangzhou, China. His research interest focuses on power simulation and control engineering.

Shouyan Chen received the B.Eng. degree in process control and the Ph.D. degree in mechanical design from the South China University of Technology, Guangzhou, China, in 2008 and 2017, respectively.

He is currently an Associate Professor with the School of Mechanical and Electrical Engineering, Guangzhou University, Guangzhou. His research interests include robotics, human–robot interaction, and intelligent control.

Limin Wang received the Ph.D. degree in operations research and cybernetics from the Dalian University of Technology, Dalian, China, in 2009.

She is currently a Professor with the School of Mechanical and Electrical Engineering, Guangzhou University, Guangzhou, China.

Zhijia Zhao (Member, IEEE) received the B.Eng. degree in automatic control from North China University of Water Resources and Electric Power, Zhengzhou, China, in 2010, and the M.Eng. and Ph.D. degrees in automatic control from South China University of Technology, Guangzhou, China, in 2013 and 2017, respectively.

He is currently an Associate Professor with the School of Mechanical and Electrical Engineering, Guangzhou University, Guangzhou. His research interests include adaptive and learning control, flexible mechanical systems, and robotics.

Zhijie Liu (Member, IEEE) received the B.Sc. degree in automatic control from the China University of Mining and Technology Beijing, Beijing, China, in 2014, and the Ph.D. degree in automatic control from Beihang University, Beijing, in 2019.

In 2017, he was a Research Assistant with the Department of Electrical Engineering, University of Notre Dame, Notre Dame, IN, USA, for 12 months. He is currently a Professor with the School of Intelligence Science and Technology, University of Science and Technology Beijing, Beijing. His research interests include adaptive control, modeling and vibration control for flexible structures, and distributed parameter systems.

Keum-Shik Hong (Life Fellow, IEEE) received the B.S. degree in mechanical design from Seoul National University, Seoul, South Korea, in 1979, the M.S. degree in mechanical engineering from Columbia University, New York, NY, USA, in 1987, and the M.E. degree in applied mathematics and the Ph.D. degree in mechanical engineering from the University of Illinois at Urbana–Champaign, Champaign, IL, USA, in 1991 and 1997, respectively.

He joined the School of Mechanical Engineering, Pusan National University, Busan, South Korea, in 1993. His research interests include brain–computer interface, nonlinear systems theory, adaptive control, and distributed parameter systems.

Dr. Hong has received many awards, including the Best Paper Award from the KFSTS of Korea in 1999 and the Presidential Award of Korea in 2007. He served as an Associate Editor for *Automatica* from 2000 to 2006, as the Editor-in-Chief for the JOURNAL OF MECHANICAL SCIENCE AND TECHNOLOGY from 2008 to 2011, and the Editor-in-Chief for the *International Journal of Control, Automation, and Systems*. He was the Past President of the Institute of Control, Robotics and Systems (ICROS), Seoul, South Korea, and the President of the Asian Control Association. He is a Fellow of the Korean Academy of Science and Technology, an ICROS Fellow, and a member of the National Academy of Engineering of Korea.